## SUPPORTING INFORMATION

-----

## Molecular ink-based synthesis of Bi(S<sub>z</sub>Se<sub>1-z</sub>)(I<sub>x</sub>Br<sub>1-x</sub>) solid solutions as tuneable materials for sustainable energy applications

<u>D. Rovira<sup>1,2</sup></u>, I. Caño<sup>1,2</sup>, C. López<sup>2,3</sup>, A. Navarro-Güell<sup>1,2</sup>, J.M. Asensi<sup>4,5</sup>, L. Calvo-Barrio<sup>6,7</sup>, L. Garcia-Carreras<sup>6</sup>, X. Alcobe<sup>6</sup>, L. Cerqueira<sup>8</sup>, V. Corregidor<sup>8</sup>, Y. Sanchez<sup>9</sup>, A. Jimenez-Arguijo<sup>1,2</sup>, O. El Khouja<sup>1,2</sup>, S. Lanzalaco<sup>2,12</sup>, J. W. Turnley<sup>10,11</sup>, R. Agrawal<sup>10</sup>, C. Cazorla<sup>2,3</sup>, J. Puigdollers<sup>1,2</sup>, E. Saucedo<sup>1,2</sup>

**Table S1.** Specification of precursor ratios for each Bi-chalcohalide compound. The values presented correspond to the ratio  $Bi(NO_3)_3 \cdot 5H_2O : SC(NH_2)_2 : SeC(NH_2)_2 : BiI_3 : BiBr_3 . X$  denotes the proportion of Bi-precursor salt that corresponds to bismuth nitrate,  $X \in [0,1]$ .

	Bi(NO₃)₃•5H₂O	$SC(NH_2)_2$	$SeC(NH_2)_2$	Bil₃	BiBr₃
BiSI	X	1	-	1-X	-
BiSI <sub>0.7</sub> Br <sub>0.3</sub>	X	1	-	0.7(1-X)	0.3(1-X)
$BiSI_{0.5}Br_{0.5}$	X	1	-	0.5(1-X)	0.5(1-X)
$BiSI_{0.3}Br_{0.7}$	X	1	-	0.3(1-X)	0.7(1-X)
BiSBr	X	1	-	-	(1-X)
BiS <sub>0.7</sub> Se <sub>0.3</sub> Br	X	0.7	0.3	-	(1-X)
BiS <sub>0.5</sub> Se <sub>0.5</sub> Br	X	0.5	0.5	-	(1-X)
BiS <sub>0.3</sub> Se <sub>0.7</sub> Br	X	0.3	0.7	-	(1-X)
BiSeBr	X	-	1	_	(1-X)
BiSel	X	-	1	(1-X)	-

<sup>&</sup>lt;sup>1</sup>Universitat Politècnica de Catalunya (UPC), Photovoltaic Lab – Micro and Nano Technologies Group (MNT), Electronic Engineering Department, EEBE, Av Eduard Maristany 10-14, Barcelona 08019, Spain

<sup>&</sup>lt;sup>2</sup>Universitat Politècnica de Catalunya (UPC), Barcelona Centre for Multiscale Science & Engineering, Av Eduard Maristany 10-14, Barcelona 08019, Spain

<sup>&</sup>lt;sup>3</sup>Universitat Politècnica de Catalunya (UPC), Group of Characterization of Materials (GCM), Physics Department, EEBE, Av Eduard Maristany 10-14, Barcelona 08019, Spain

<sup>&</sup>lt;sup>4</sup>Universitat de Barcelona (UB), Applied Physics Department, C. Martí I Franquès 1, Barcelona 08028, Spain

<sup>&</sup>lt;sup>5</sup>Institute of Nanoscience and Nanotechnology (IN2UB), Universitat de Barcelona, 08028 Barcelona, Spain.

<sup>&</sup>lt;sup>6</sup>Universitat de Barcelona (UB), Scientific and Technological Centers (CCiTUB), C. Lluís Solé i Sabaris 1-3, Barcelona 08028, Spain

<sup>&</sup>lt;sup>7</sup>Universitat de Barcelona (UB), Electronics and Biomedical Engineering Department, C. Martí I Franquès 1, Barcelona 08028, Spain <sup>8</sup>Centro de Ciências E Tecnologias Nucleares (C2TN), Instituto Superior Técnico, Universidade de Lisboa, E.N. 10 Ao Km 139.7, 2695-066, Bobadela LRS, Portugal

<sup>°</sup>Catalonia Institute for Energy Research – IREC, Jardins de les Dones de Negre 1, Sant Adrià de Besòs 08930, Spain

<sup>&</sup>lt;sup>10</sup>Davidson School of Chemical Engineering, Purdue University, West Lafayette, Indiana 47907, USA

<sup>&</sup>lt;sup>11</sup>Department of Chemical Engineering and Materials Science, Michigan State University, East Lansing, Michigan 48824, USA

<sup>&</sup>lt;sup>12</sup>Universitat Politècnica de Catalunya, Innovation in Materials and Molecular Engineering (IMEM), Department of Chemical Engineering, Av Eduard Maristany 10-14, Barcelona 08019, Spain

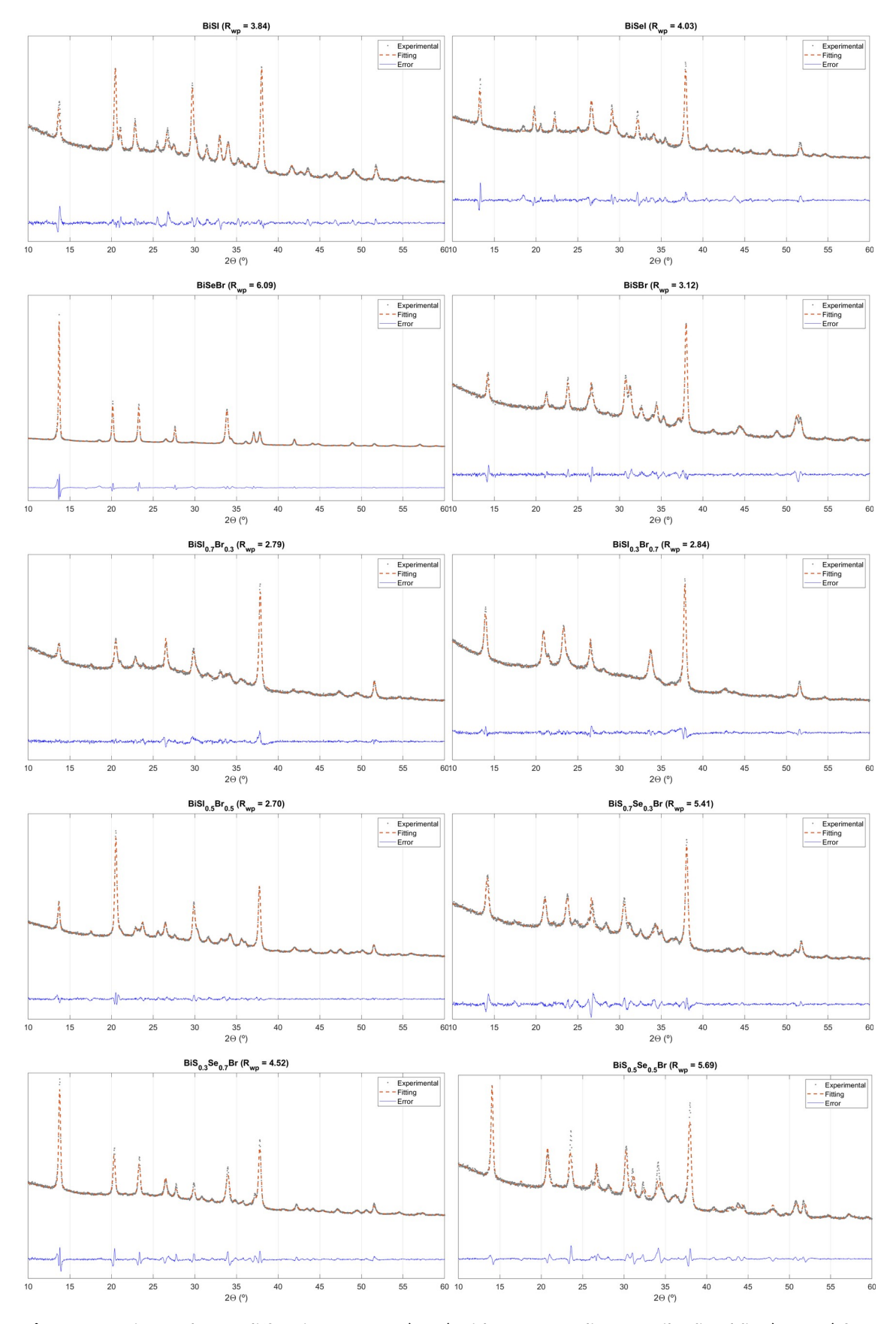


**Fig. S1.** Experimental X-ray diffraction patterns (grey) with corresponding Le Bail refined fits (orange) for all Bi-chalcohalide solid solutions. The difference between experimental and calculated profiles is shown in blue. The weighted profile R-factor ( $R_{wp}$ ) for each refinement is indicated in the respective graph titles.

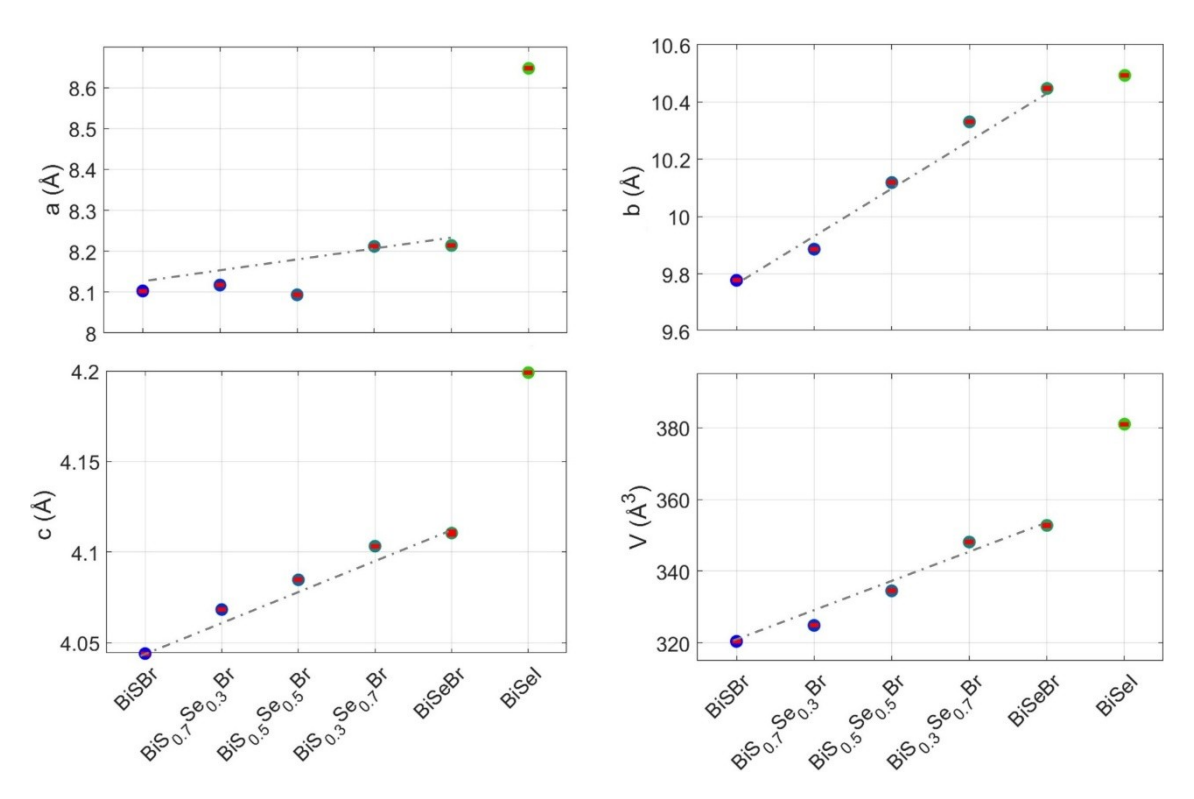


**Fig. S2.** Cell parameters and unit cell volume for the chalcogen solid solutions in Bi-chalcohalides. The dashed line indicates the theoretical evolution following Vegard's Rule. Error bars shown in red.

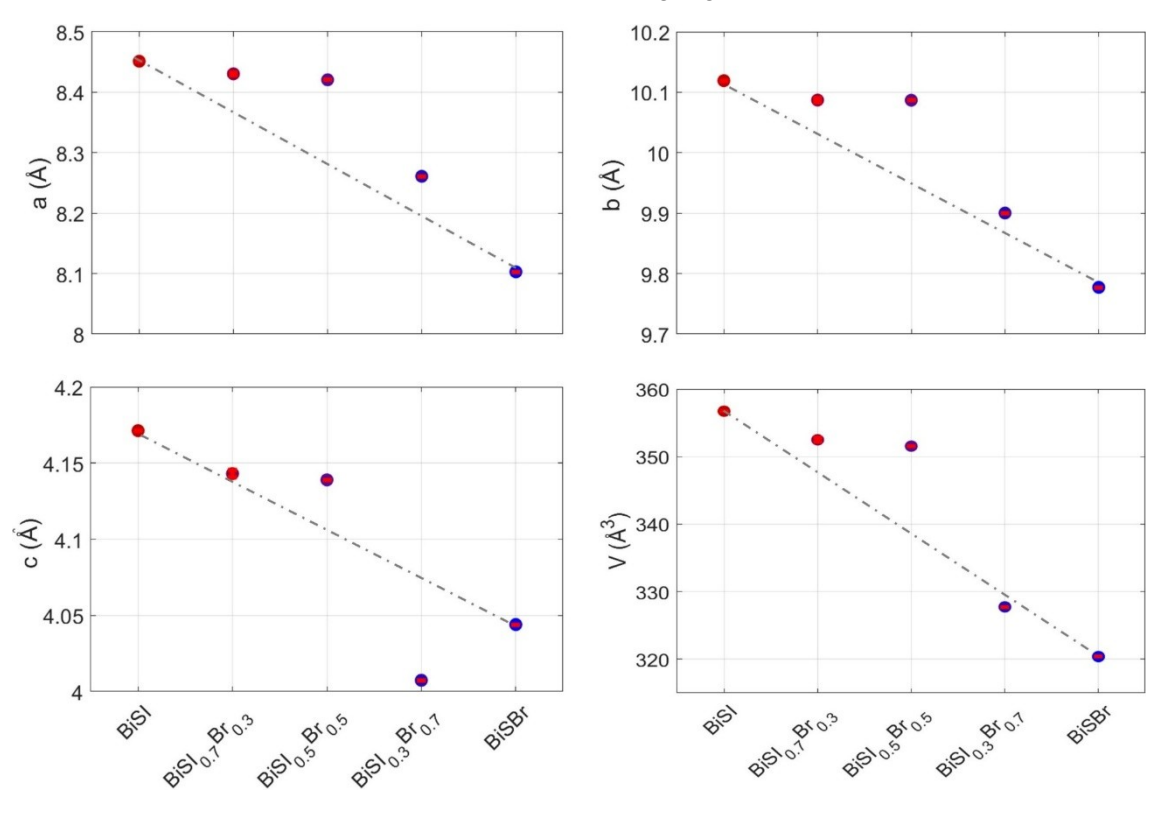


**Fig. S3.** Cell parameters and unit cell volume for the halogen solid solutions in Bi-chalcohalides. The dashed line indicates the theoretical evolution following Vegard's Rule. Error bars shown in red.

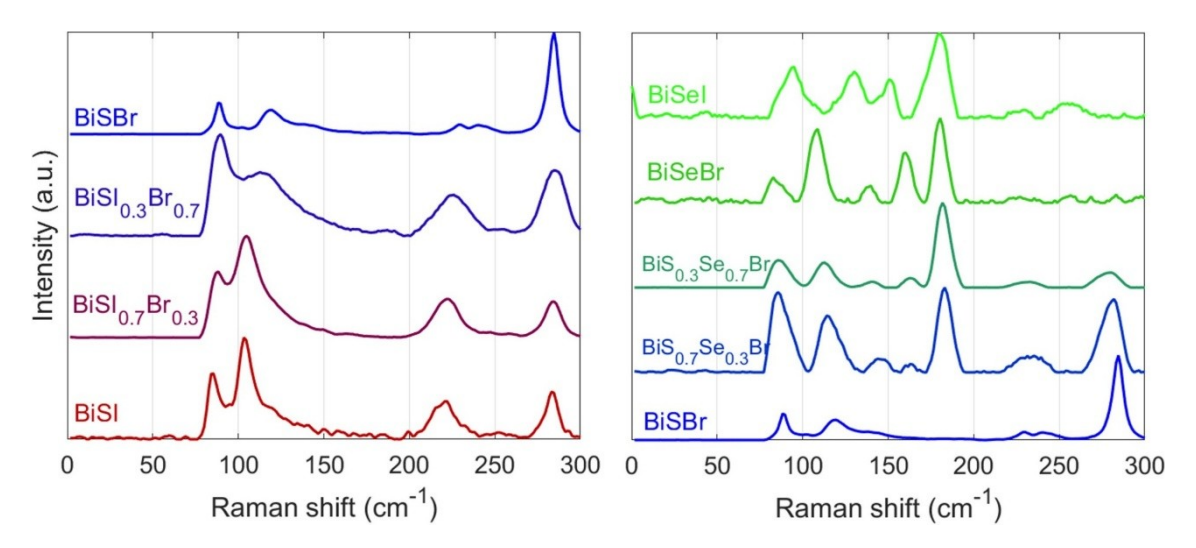
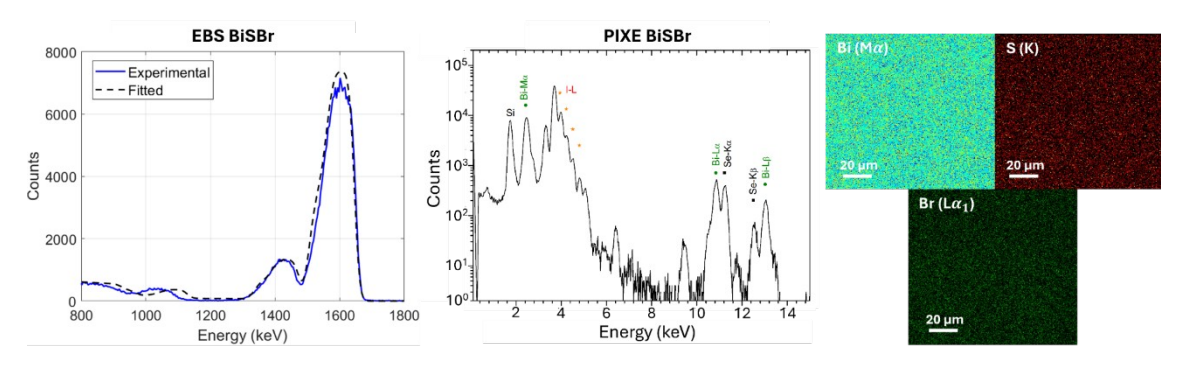
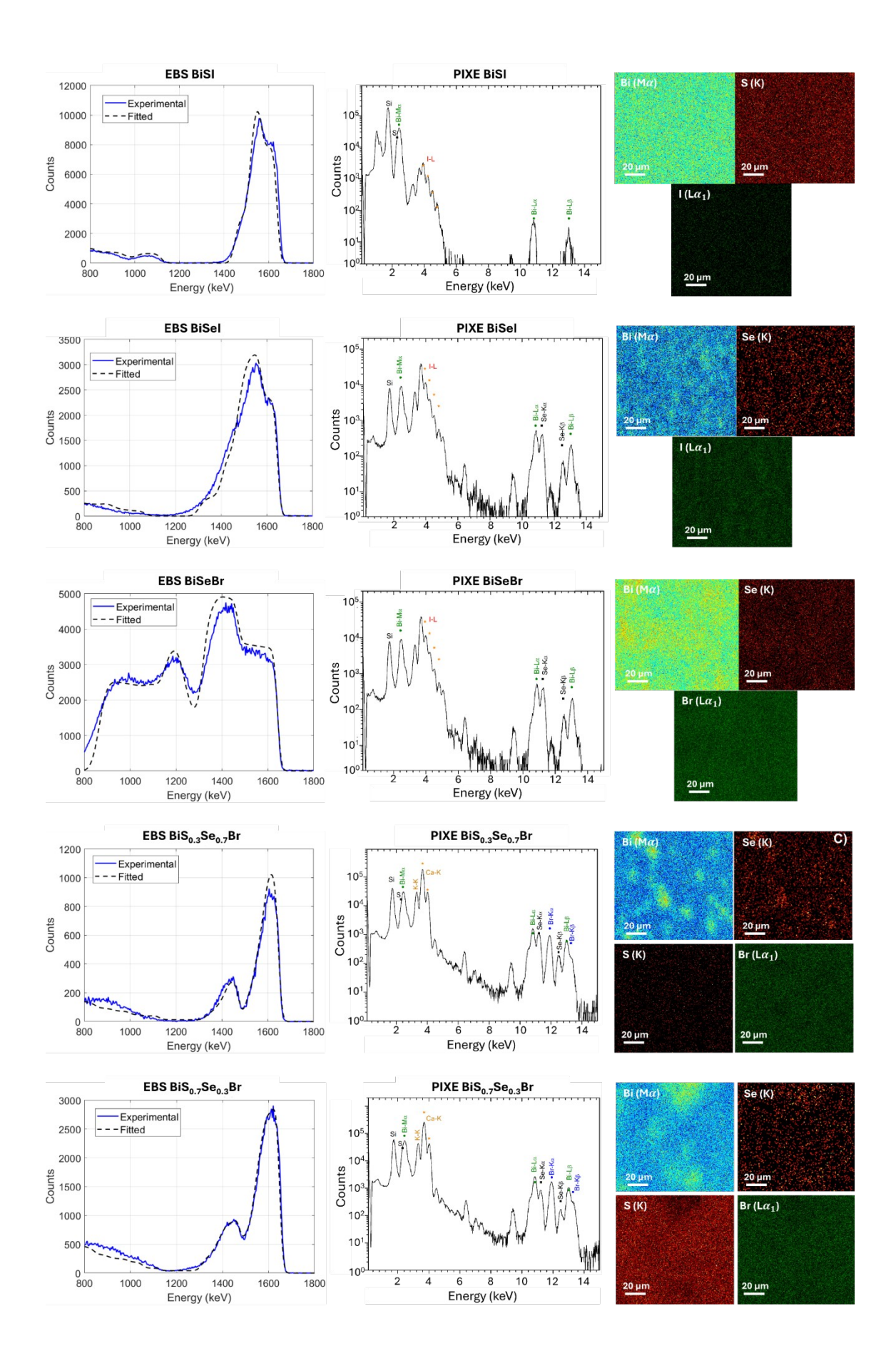


Fig. S4. Raman spectra for Bi-chalcohalide solid solutions excited with a 532 nm laser.

## **IBA Analysis**

The EBS fitting was performed considering the columnar morphology of these compounds. Due to film deposition on substrates with weaker adhesion, such as SLG or FTO, the films exhibited lower compactness compared to those grown on other substrates. This aspect is further discussed in the Morphology Control section. As a result, instead of forming a fully compact film, the material exhibits a rod-like dispersion with empty spaces at the substrate interface (see Fig. S19). Consequently, the conventional approach of modelling the EBS spectrum as a simple layered stack (e.g., SLG/BiSI) was not applicable. Instead, the porosity of the active layer at the interface had to be considered. This porosity leads to reduced shadowing of the substrate's backscattered particles, causing the substrate signal to appear more pronounced in regions where the rods create more voids. Since the detected signal represents an average over areas with varying porosity, the EBS spectrum was fitted using a multilayer stack model of the form: SLG / (SLG)<sub>0.95</sub>(BiSI)<sub>0.05</sub> /... / (SLG)<sub>1-y</sub>(BiSI)<sub>y</sub> / ... / (SLG)<sub>0.05</sub>(BiSI)<sub>0.95</sub> / BiSI, with y  $\in$  [0,1]. When extended to an infinite number of layers, this approach effectively translates the interface porosity into a composition gradient in the EBS spectrum, resembling interlayer diffusion. Additionally, porosity leads to a reduction in the effective thickness of the layer as measured by EBS. Although cross-sectional scanning electron microscope (SEM) views (Fig. S19) indicates a film thickness of approximately 500 nm, the effective thickness interacting with backscattered particles in the EBS characterization is below 300 nm, as it depends on the total mass of material rather than the physical thickness alone.





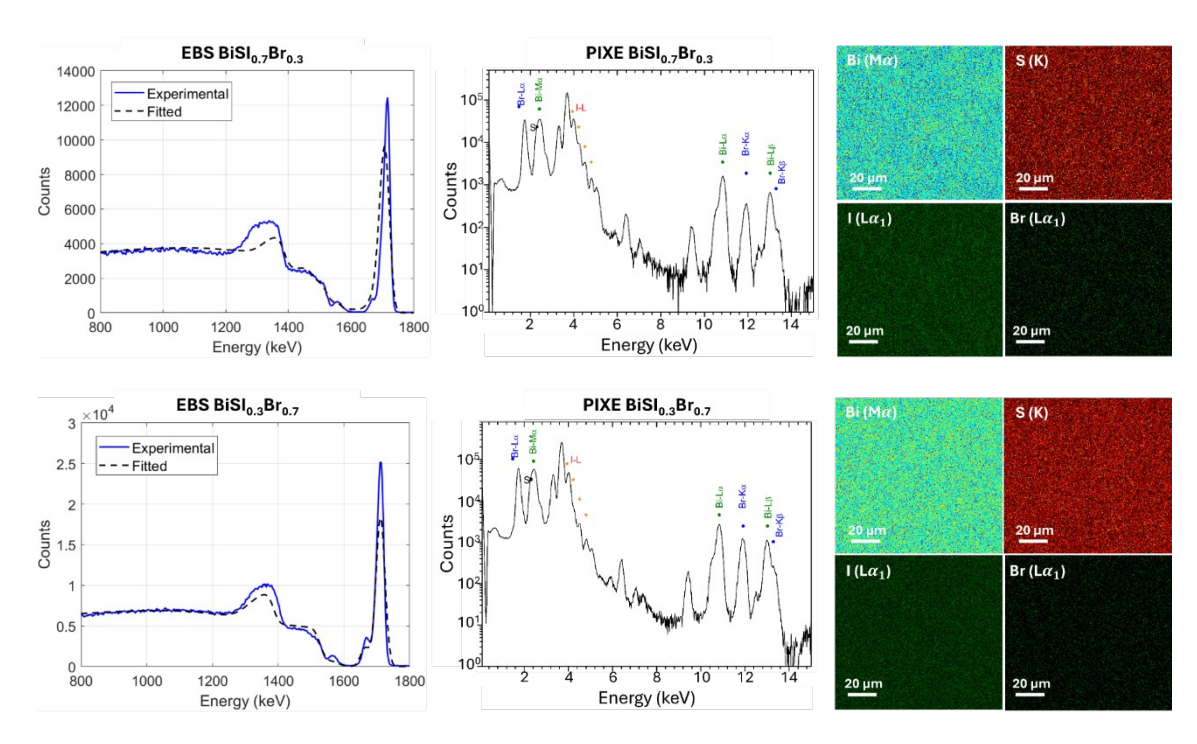


**Fig. S5.** From left to right: EBS spectra (experimental and fitted), PIXE spectra with main elemental peaks labeled, and corresponding elemental maps for Bi-chalcohalide films on glass.

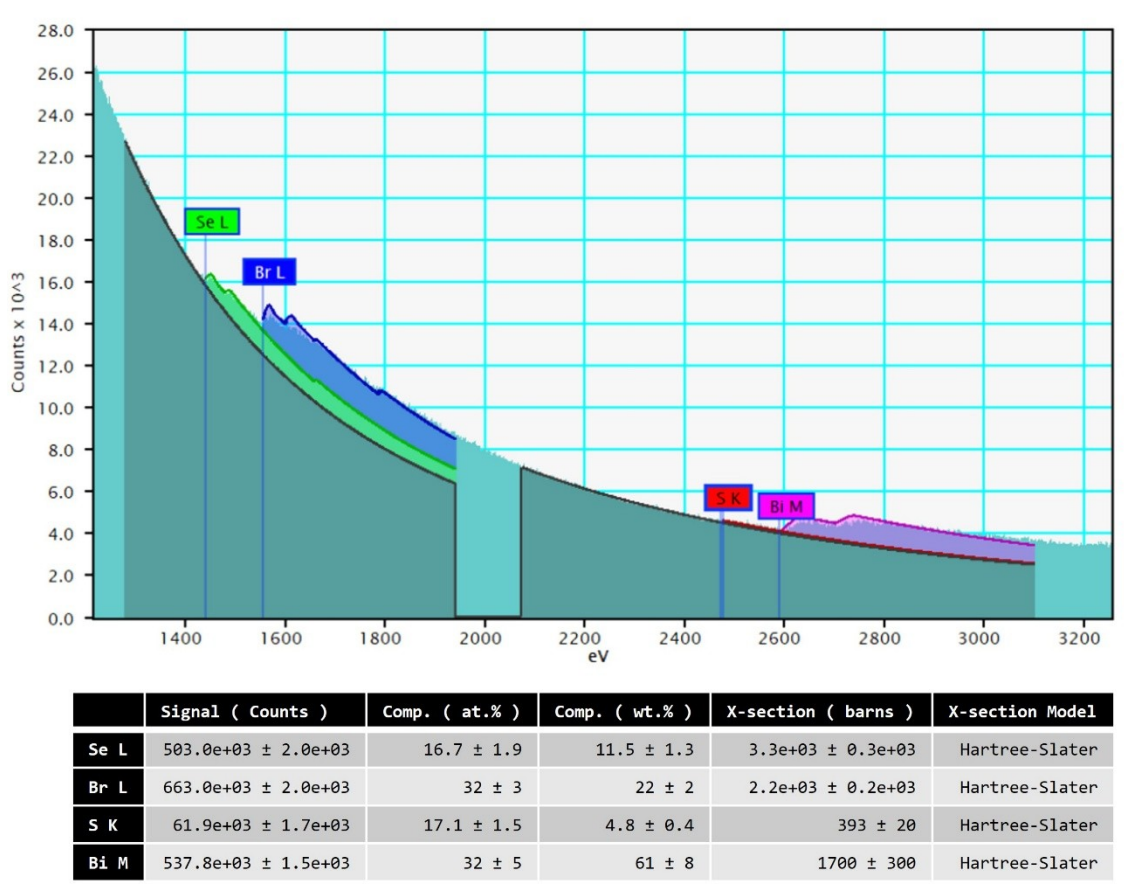


Fig. S6. EELS spectrum with elemental quantification for BiS<sub>0.5</sub>Se<sub>0.5</sub>Br.

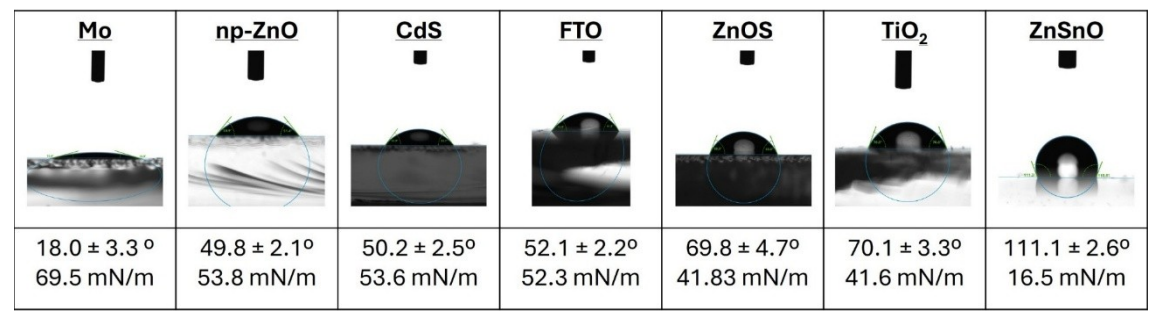
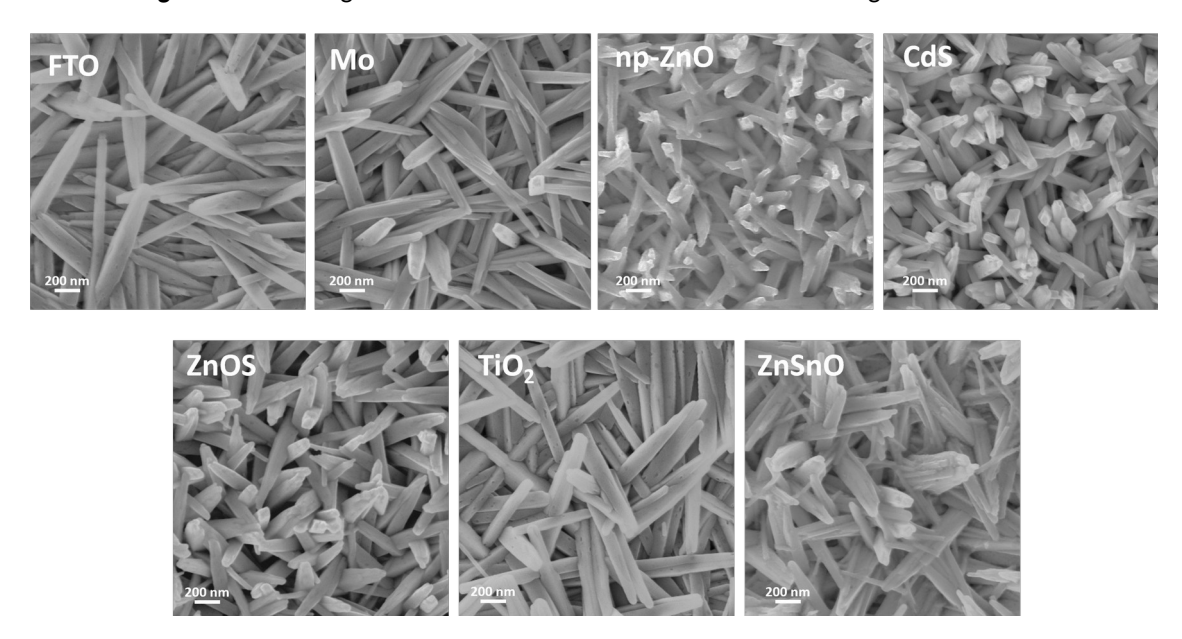


Fig. S7. Contact-angle measurements for seven different substrates grown over SLG.



**Fig. S8.** Top-view SEM images of BiSBr grown over different substrates after 3 spin-coating steps with a precursor solution concentration of 0.5 M.

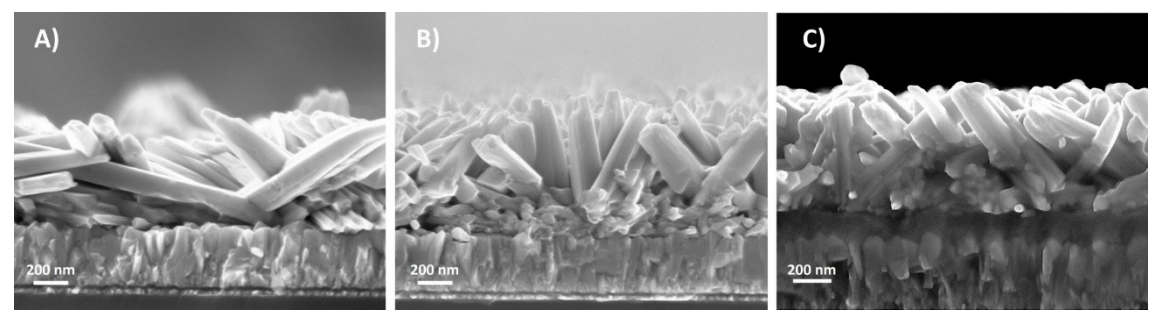


Fig. S9. Cross-section SEM images of BiSBr grown over (a) FTO/TiO<sub>2</sub>, (b) FTO/CdS and (c) FTO/ZnOS with a  $Bi(NO_3)_3$ - $5H_2O$ :  $BiX_3$  ratio of 3:2.

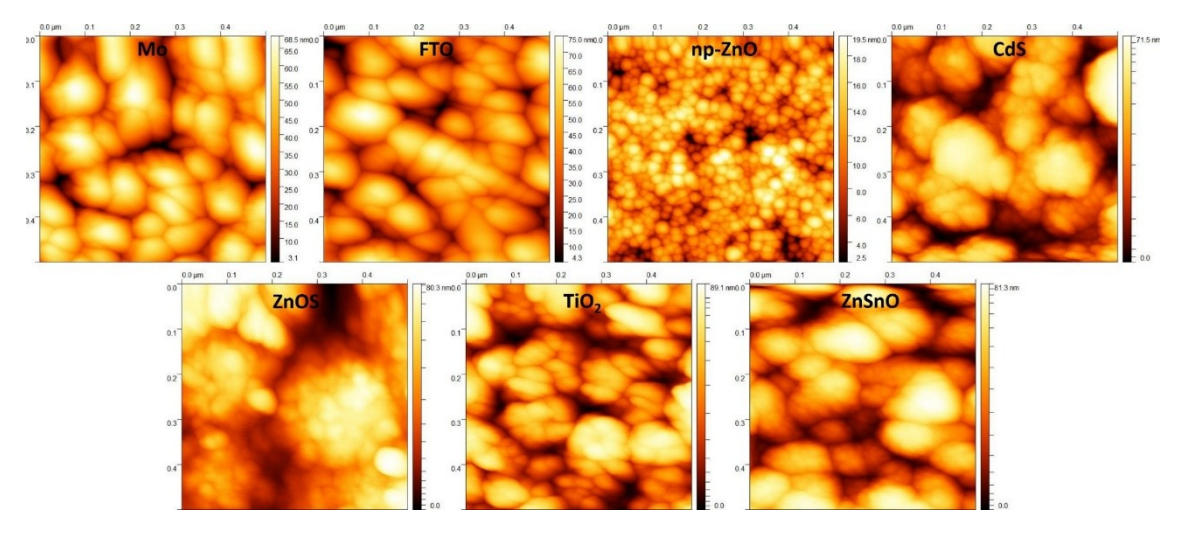


Fig. S10. AFM heigh images of different substrates used to grow Bi-chalcohalides.

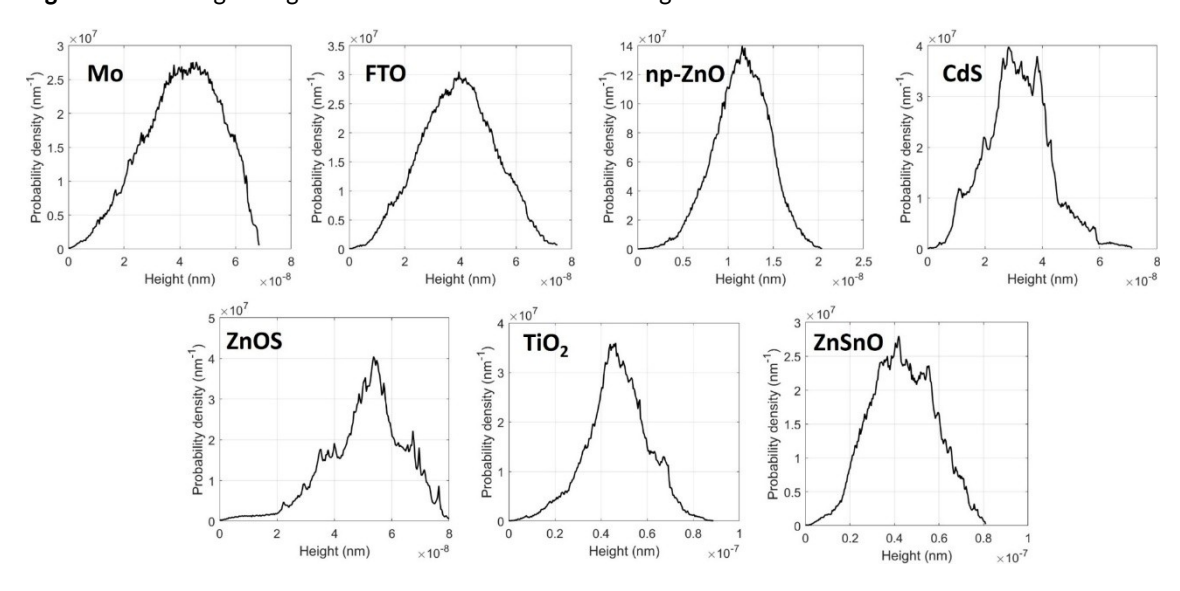
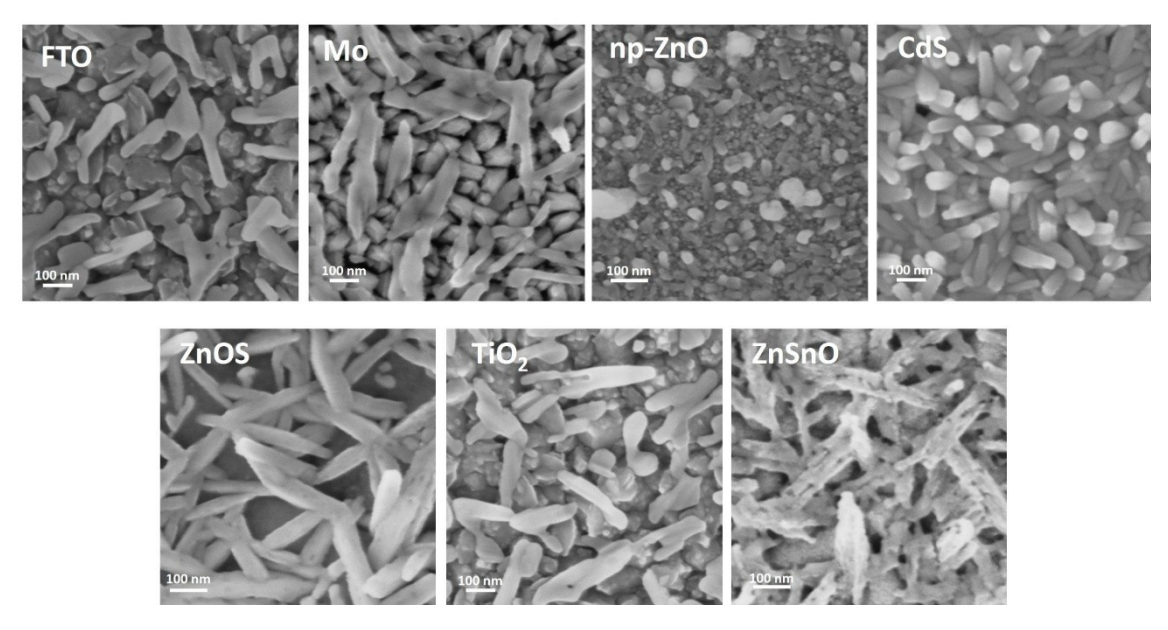
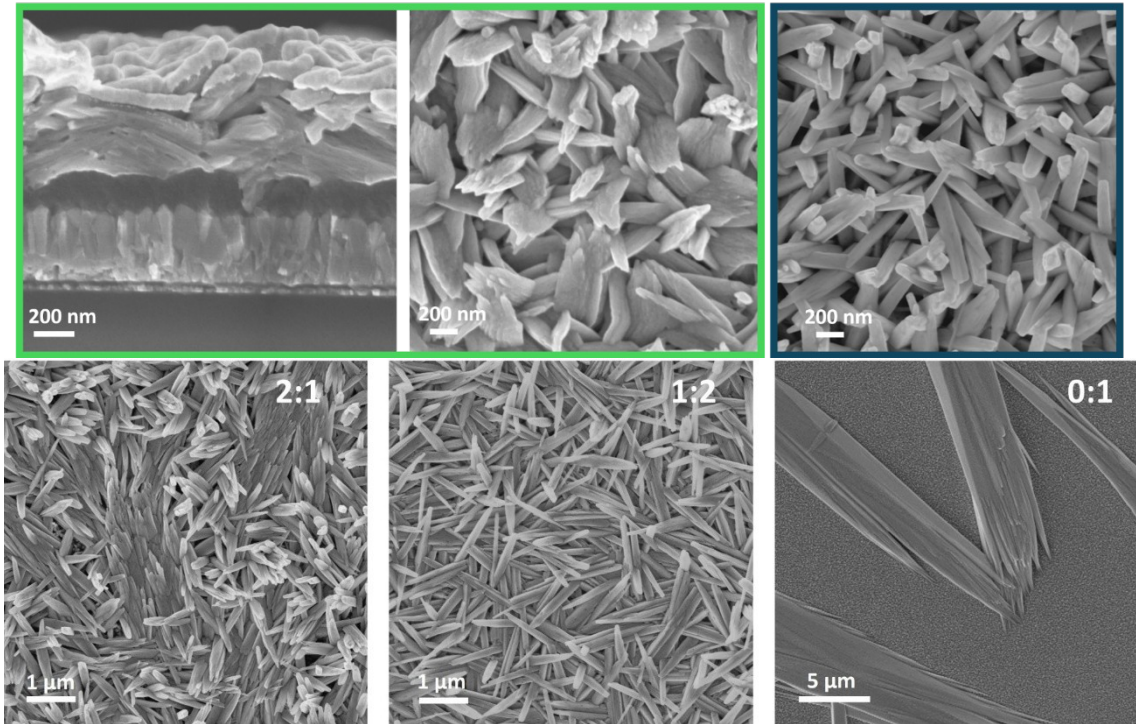


Fig. S11. Heigh distribution obtained from AFM measurements of different substrates' surface.



**Fig. S12.** Top-view SEM images of BiSBr grown over different substrates after 3 spin-coating steps using a precursor solution concentration of 0.05 M.



**Fig. S13. (Top)** Top-view and cross-sectional SEM images of BiSBr grown over ZnS with different  $Bi(NO_3)_3 \cdot 5H_2O$ :  $BiX_3$  ratios. **(Bottom)** Top-view SEM images of BiSBr grown over FTO with different  $Bi(NO_3)_3 \cdot 5H_2O$ :  $BiX_3$  ratios.

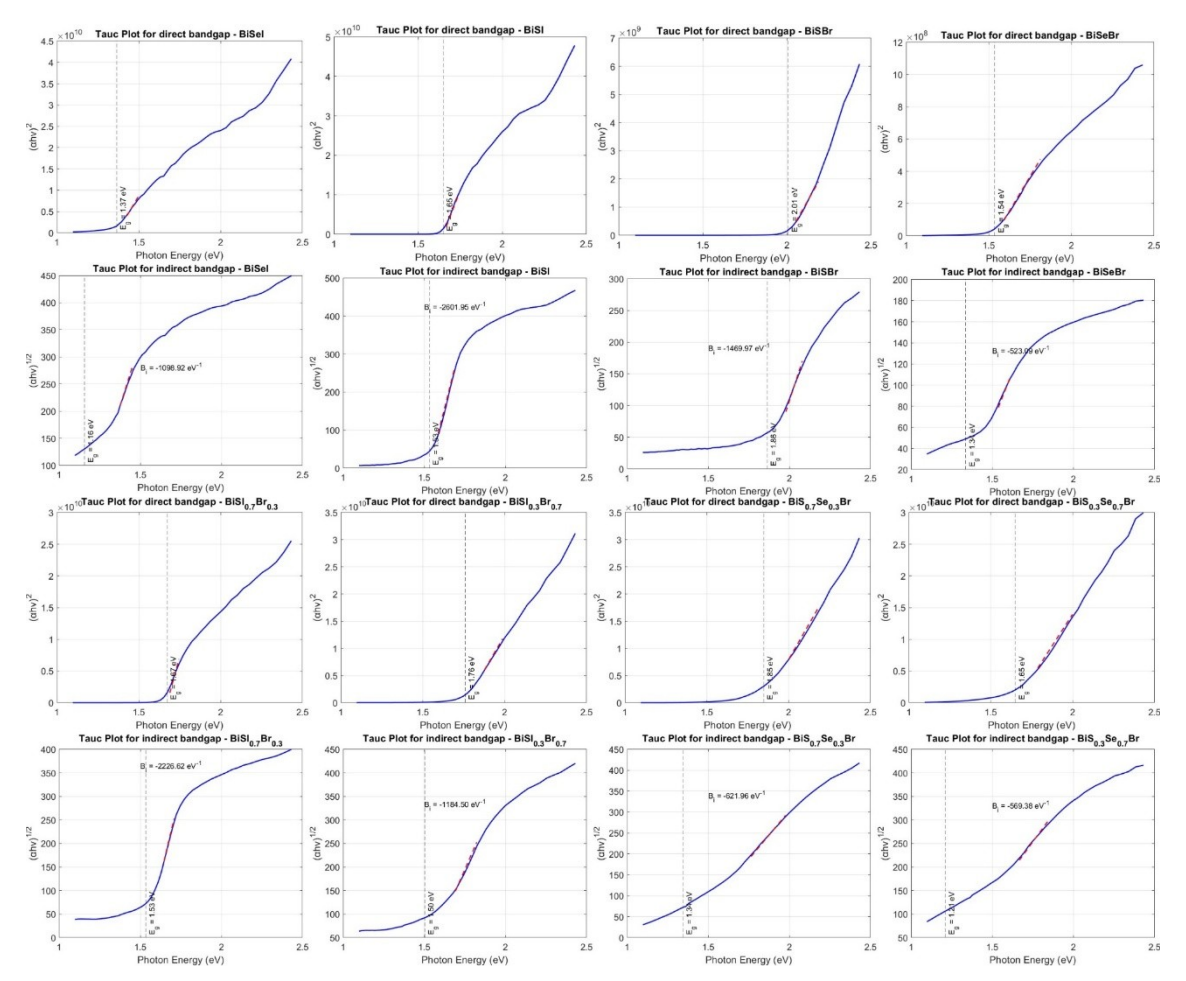


**Fig. S14.** Tauc plots for indirect and direct models from PDS absorption measurements of Bi-chalcohalide compounds.

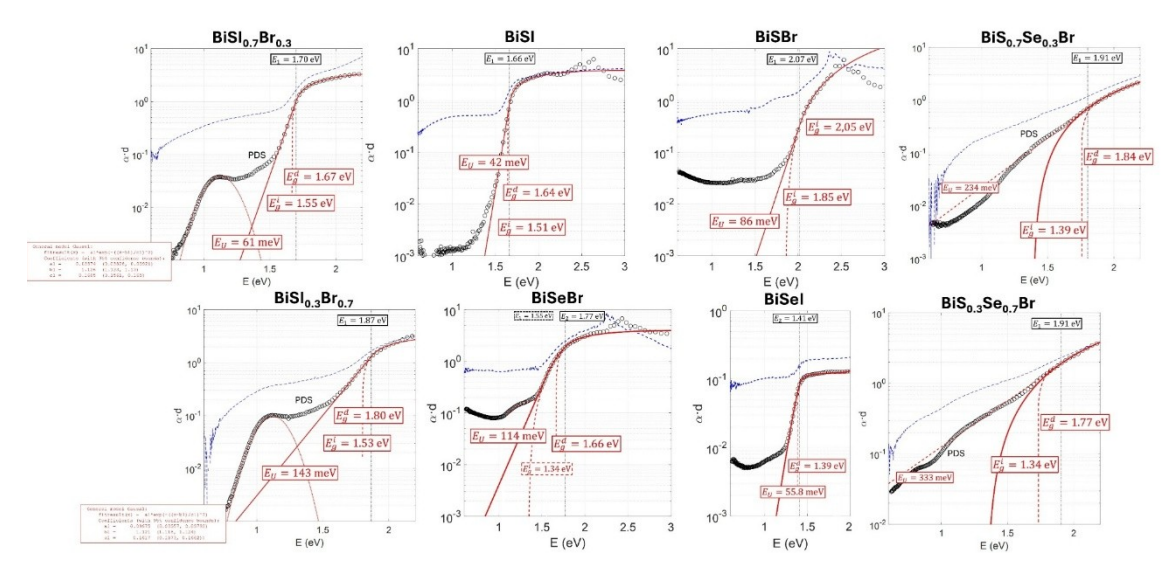


**Fig. S15.** PDS absorption fitted with Urbach-Tauc model. Experimental data in black, fitted model in red and optical absorption in blue. The values for the bandgaps and Urbach energy are displayed. For the halogen solid solutions we add the details of the gaussian fitted sub-gap discrete state.

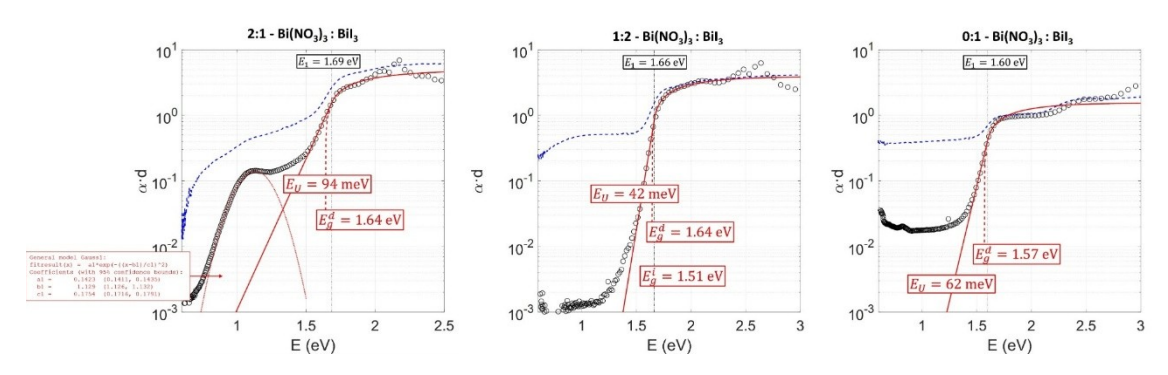


**Fig. S16.** PDS absorption for BiSI with synthesized with different content of bismuth (III) nitrate pentahydrate in the precursor molecular ink. The deposition conditions were the same for the three samples. The sub-gap absorption disappears when the content of nitrate decreases.

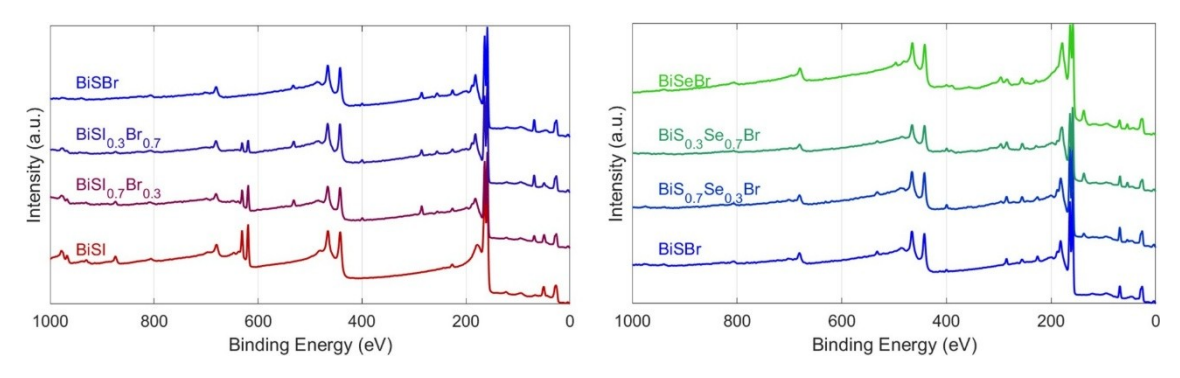


Fig. S17. XPS spectra for Bi-chalcohalide samples.

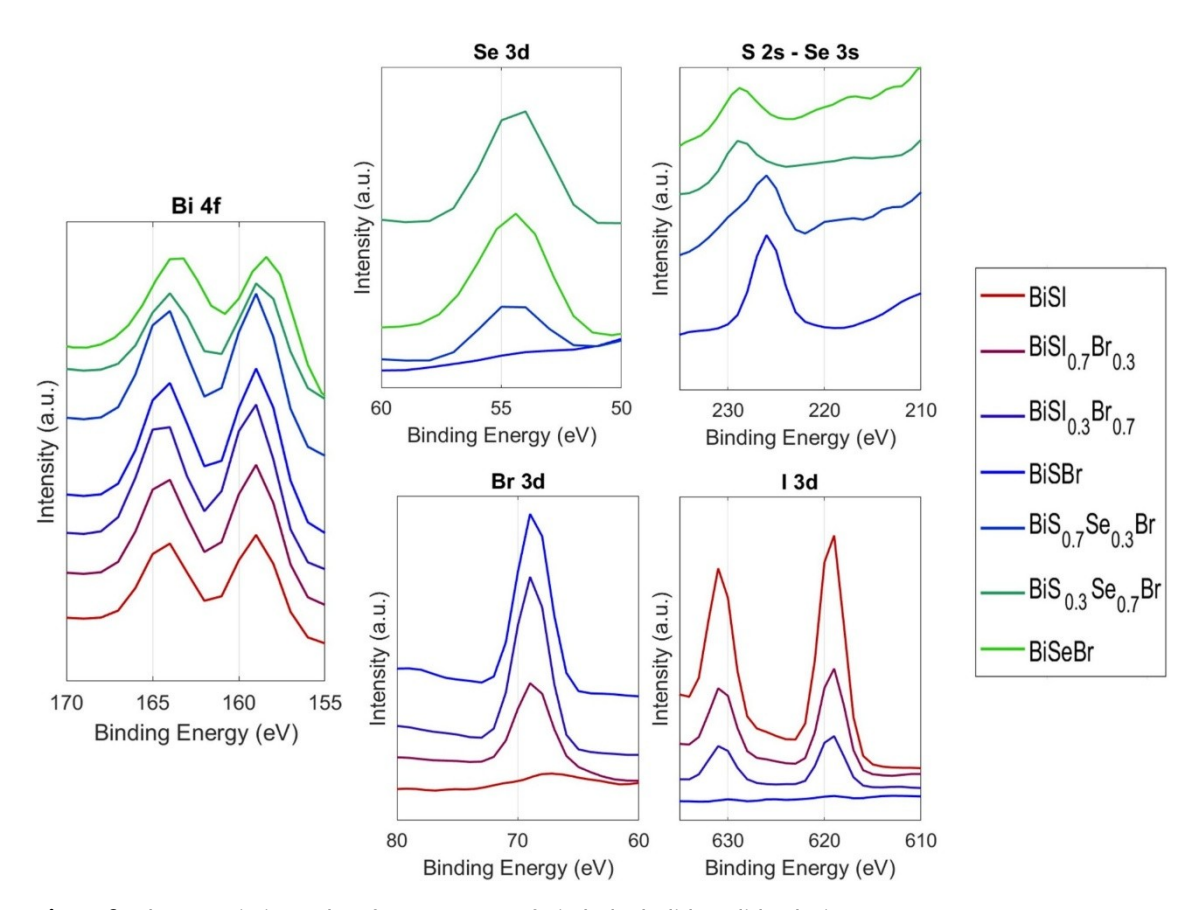
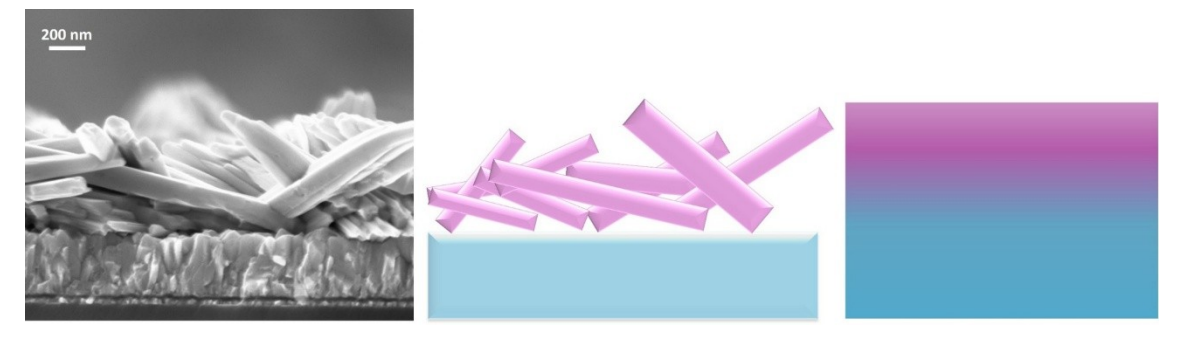


Fig. S18. Characteristic peaks of XPS spectra of Bi-chalcohalide solid solutions.



**Fig. S19.** SEM cross-sectional view of the BiSI parent compound on an FTO substrate (**left**). Schematic representation of the chalcohalide nanorod arrangement, illustrating the void spaces at the substrate interface (**centre**). Graphical depiction of the interface concentration gradient observed in EBS measurements, attributed to film porosity (**right**).